Simulation of the internetwork chromosphere

Damien Przybylski[1,*], Robert H. Cameron[1], Sami K. Solanki[1,2]
*przybylski@mps.mpg.de, ORCID: 0000-0003-1670
[1]Max-Planck Institute for Solar System Research, 37077 Göttingen, Germany
[2]School of Space Research, Kyung Hee University, Yongin, Gyeonggi 446-701, Republic of Korea

MAX PLANCK INSTITUTE FOR SOLAR SYSTEM RESEARCH

Introduction: Many mechanisms have been proposed to heat the solar chromosphere; including magnetoacoustic and Alfvénic waves, spicules, and reconnection driven eruptive events. Despite this, there is not yet a detailed understanding of the importance of these different heating mechanisms. The dynamics and structure of the solar chromosphere is determined by its underlying magnetic field. The lowest magnetic state of the solar atmosphere is provided by the small-scale dynamo (SSD) process operating in the convection zone. We aim to understand the flux of energy into the chromosphere provided by SSD fields.

Simulation Setup: We perform a 3D radiative magnetohydrodynamic (rMHD) simulation using the MURaM code (Vögler et al. 2005). Rempel (2017) included the physics necessary to treat the solar corona.
A new extension, developed by Przybylski et al. (2022), includes the physics required to treat the solar chromosphere, as in Bifrost (Gudiksen et al. 2012); a non-equilibrium treatment of hydrogen ionisation (Leenaarts et al. 2007) and H_2, chromospheric cooling recipes (Carlsson & Leenaarts 2012), and a scattering multi-group radiation transfer scheme (Skartlien 2000, Hayek 2010).
We perform a simulation of 12x12 Mm horizontally, from -7 Mm below the photosphere to 13 Mm into the corona with 512x512x1200 gridpoints. The simulation is initiated with a seed field which is enhanced by the small-scale dynamo mechanism (Rempel 2014).

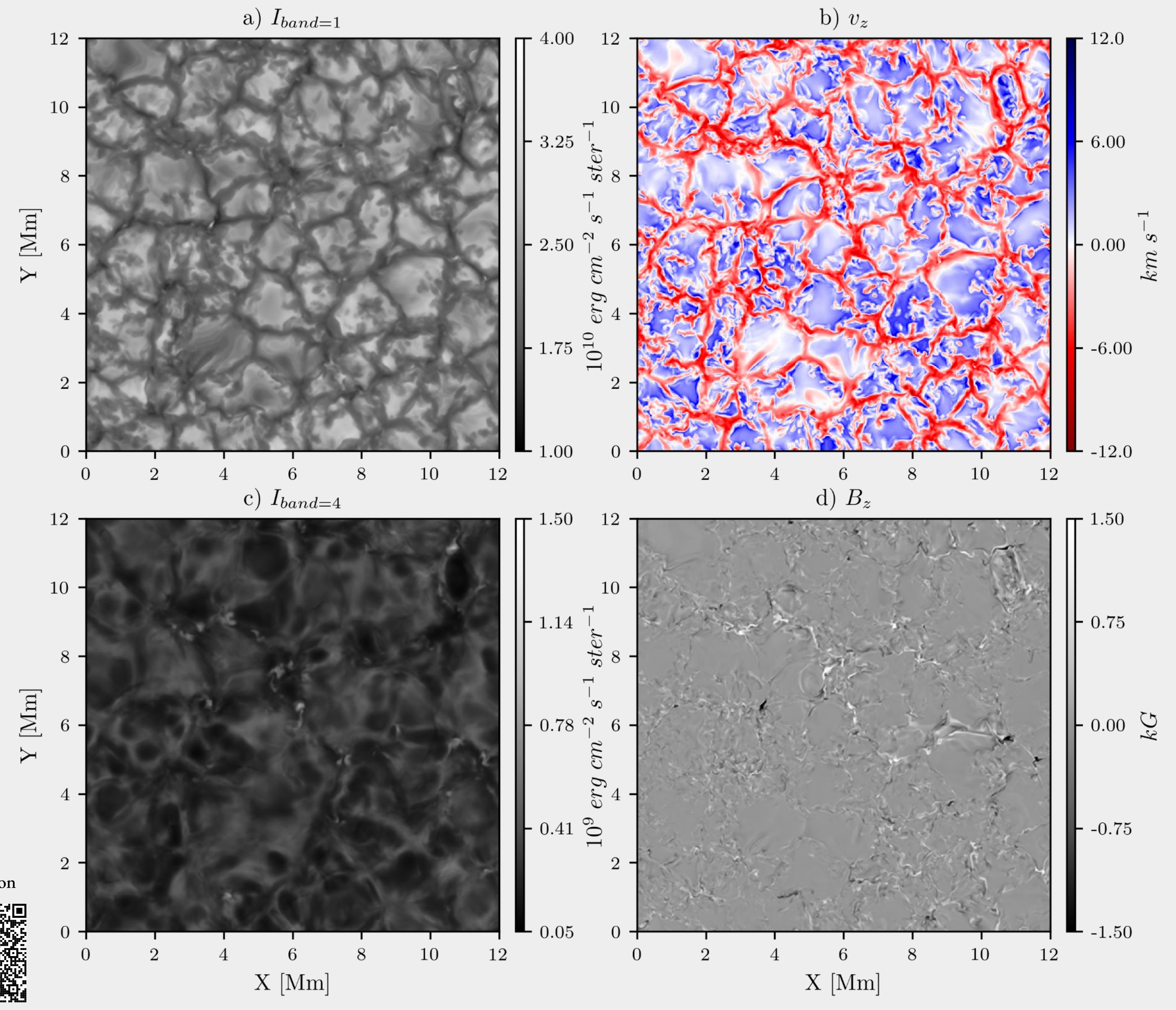

Animation

Above: The photosphere of the quiet-sun simulation.

Animation

Below: An vertical slice of the simulation, showing the chromospheric dynamics.

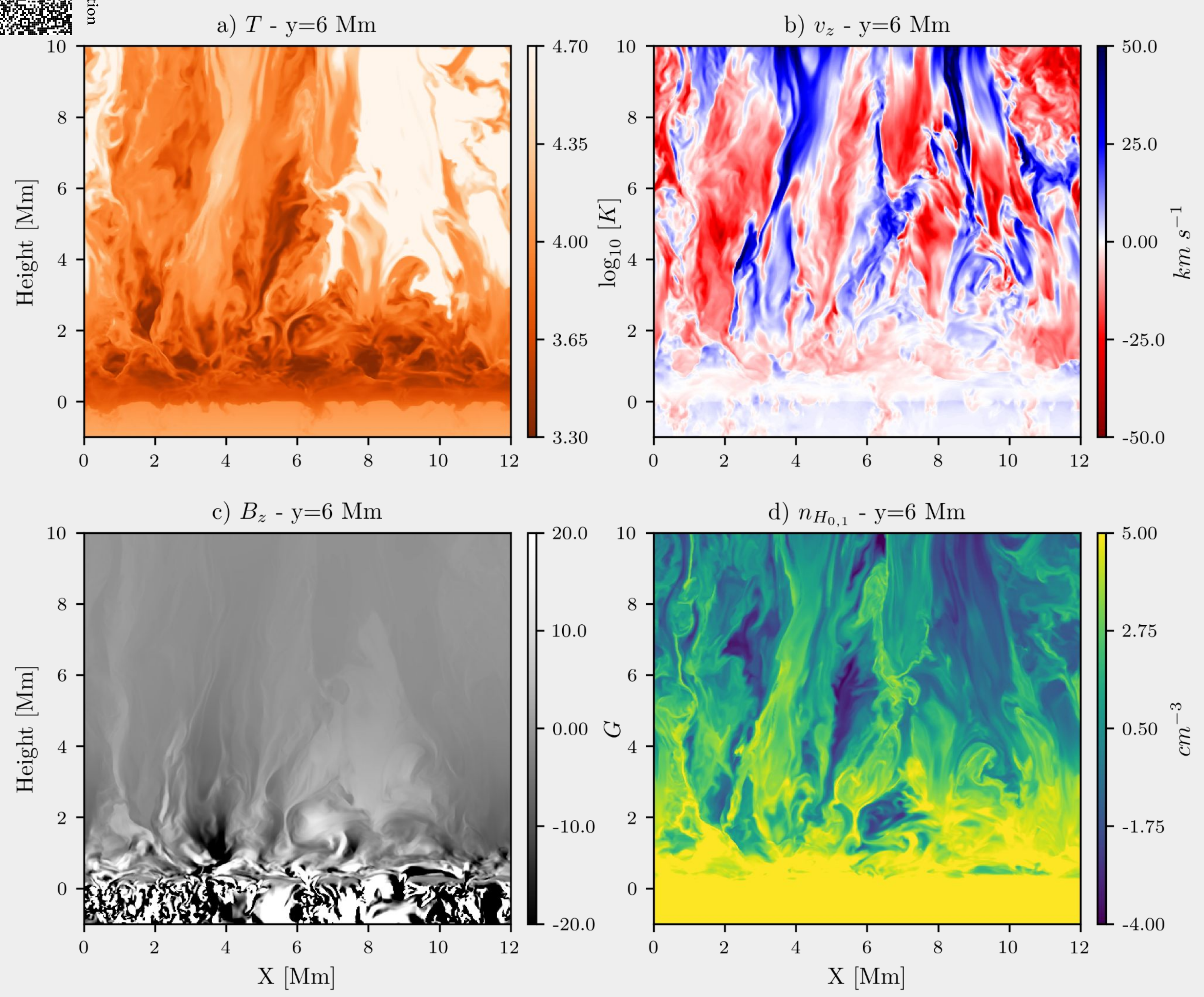

Results: The simulation develops a salt-and-pepper magnetic field with concentrations up to ≈ 2kG. The photospheric field in the time-series reaches $|B_z|_{havg}$ = 71.59 ±2.98 G, B_{rms} = 141.34±7.42 G. By the mid-chromosphere the magnetic energy dominates the kinetic. The chromosphere is highly dynamic, showing strong shocks. Although it cannot form a steady 10^6 K corona, local heating events reach over a 10^6 K.

Below: The horizontally and temporally averaged magnetic, kinetic and thermal energies.

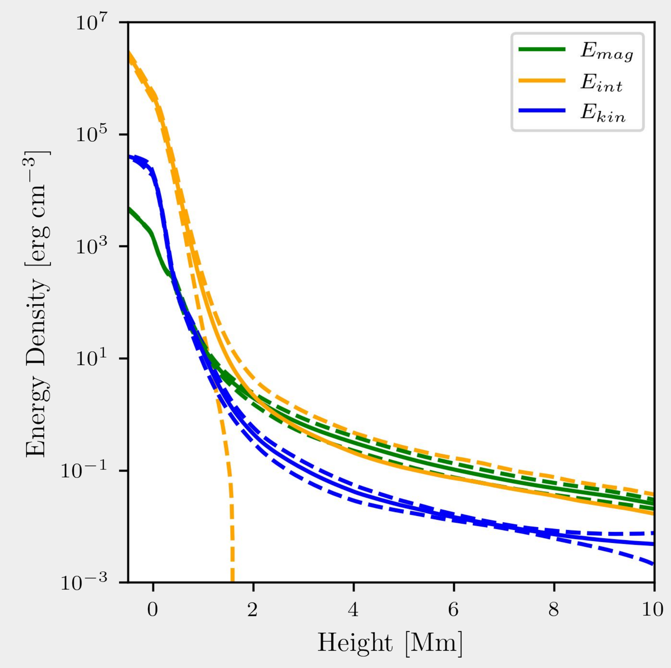

Energy Flux: The vertical Poynting flux is split into two components:

$$P_{z,v_z} = \frac{v_z}{4\pi}(b_y^2 + b_x^2) \quad , \text{ and } \quad P_{z,b_z} = -\frac{b_z}{4\pi}(b_x v_x + v_y b_y)$$

Representing vertical advection of horizontal field, and perturbations perpendicular to the vertical field. The $P_{z,bz}$ component provides the majority of the Poynting flux to the chromosphere, the $P_{z,vz}$ component alternates in sign as shocks interact with emerging flux. The spatial dependence shows the majority of the Poynting flux reaches the upper atmosphere through a few strong magnetic field concentrations.

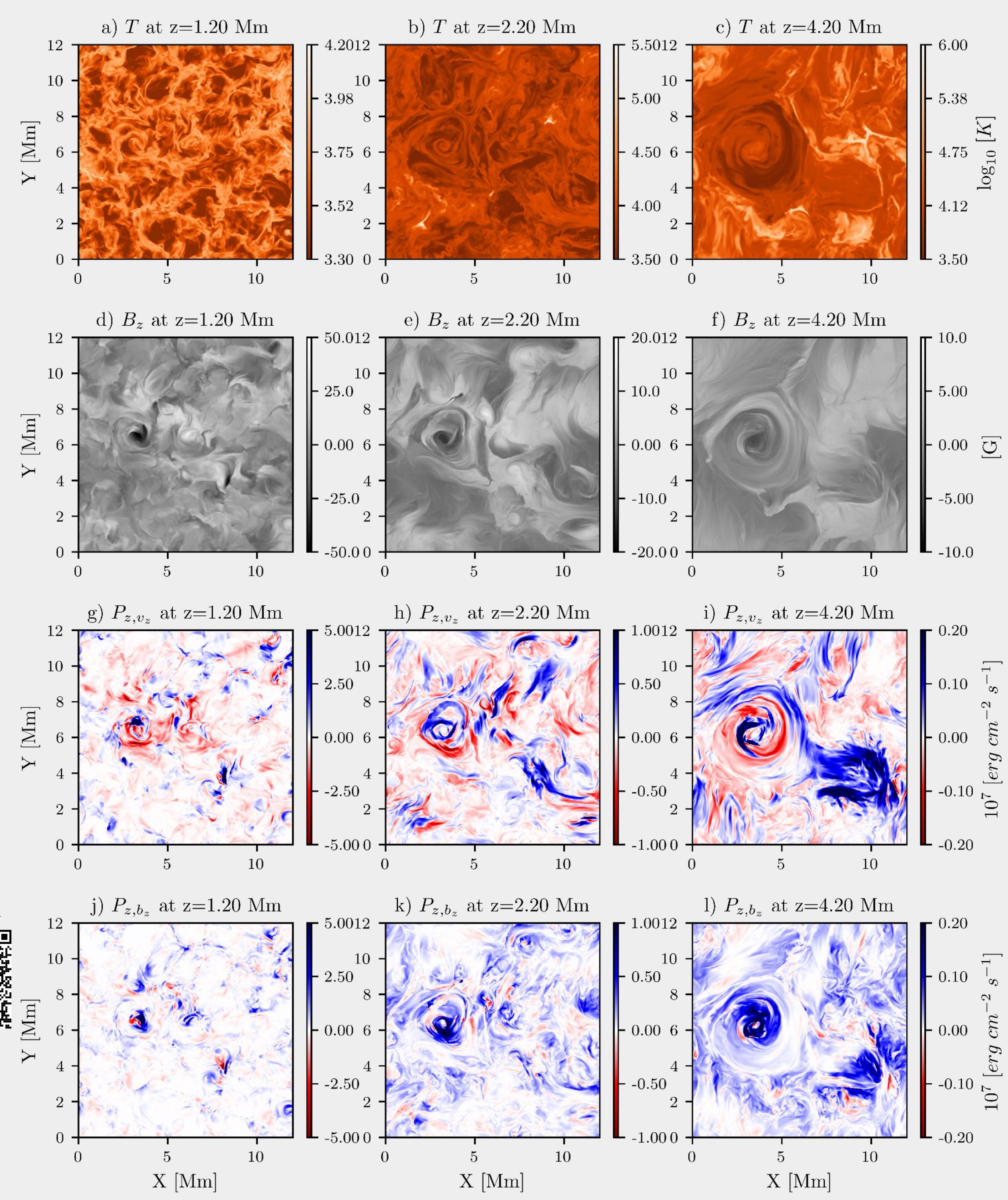

Right: Time variation of the horizontally averaged Poynting Flux.
Below: The horizontally and temporally averaged Poynting Flux.

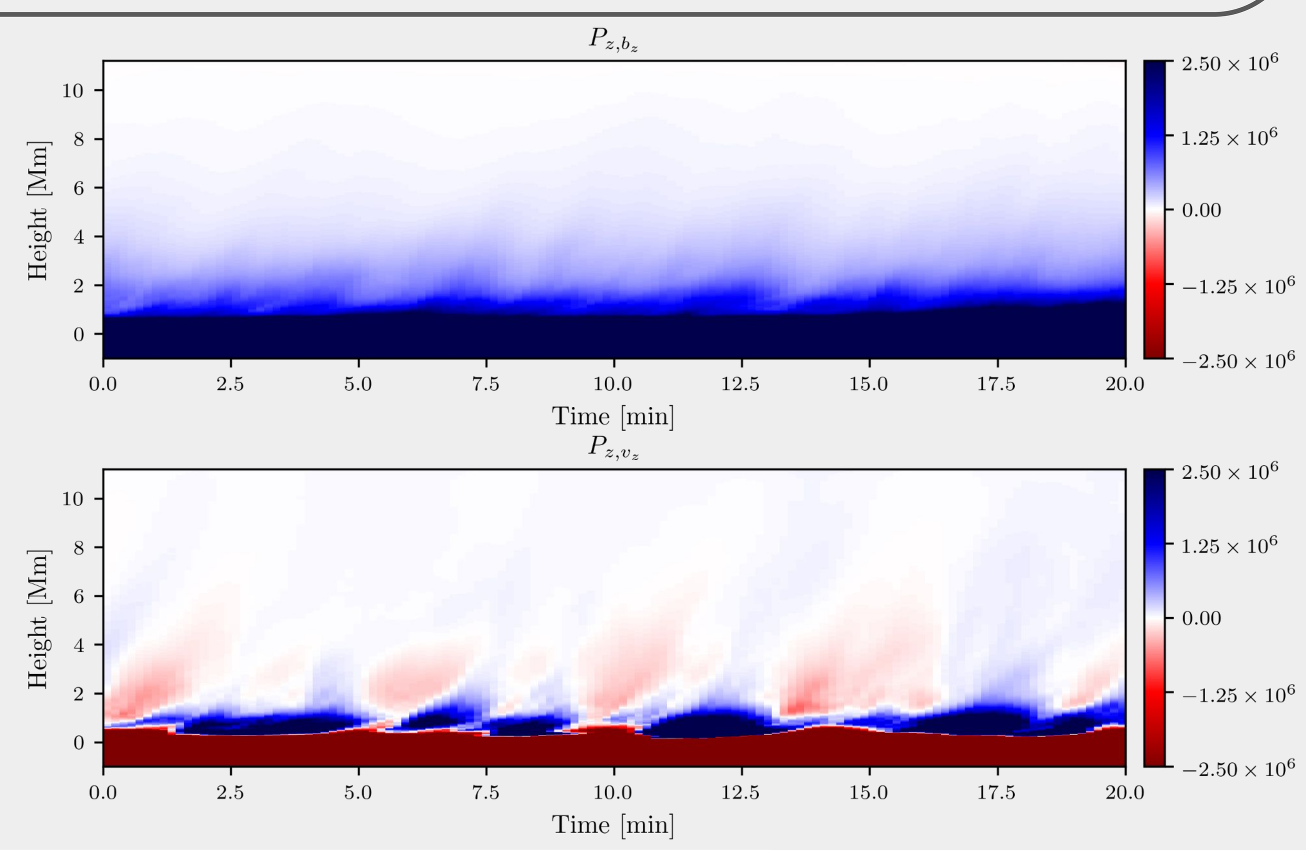

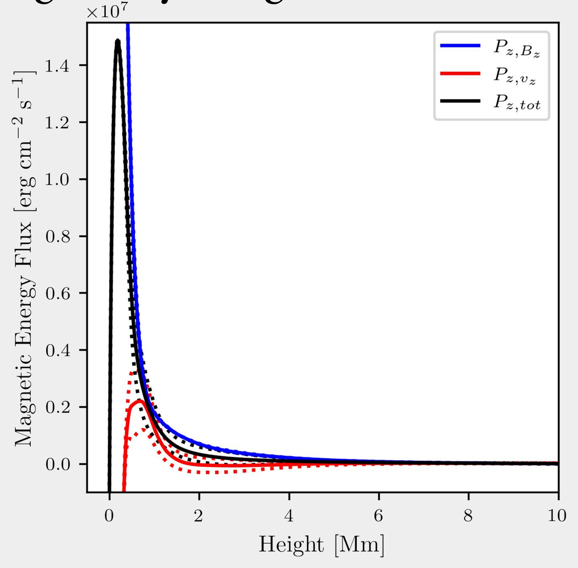

Animation

Right: The temperature, vertical magnetic field and Poynting flux at different heights in the atmosphere.

Conclusions:

- Internetwork magnetic fields are in equipartition with kinetic energy in the low-mid chromosphere and dominate by the upper chromosphere.
- These fields provide a Poynting flux approximately equal to the canonical values required to heat the quiet sun chromosphere ≈ 4×10^6 erg cm^{-2} s^{-1} (Withbroe & Noyes 1977).
- Flux emergence is an important process, however the net Poynting-flux term $P_{z,vz}$ is low, or negative in the chromosphere.
- The majority of the Poynting flux is provide by torsional motions ($P_{z,bz}$).

References:
Carlsson, M. & Leenaarts, J. 2012, A&A, 539, A39
Gudiksen, B.V., Carlsson, M., Hansteen, V.H., et al. 2011, A&A, 531, A154
Hayek, W., Asplund, M., Carlsson, M., et al. 2010, A&A, 517, A49
Leenaarts, J., Carlsson, M., Hansteen, V., & Rutten R.J. 2007, A&A, 530, A124
Przybylski, D, Cameron, R., Solanki, S.K., et al. 2022, A&A, 664, A91
Rempel, M. 2014, ApJ, 789, 132
Rempel, M. 2017, ApJ, 834, 10
Vögler, A., Shelyag, S., Schüssler, M., et al. 2005, A&A, 429,335
Withbroe, G.L. & Noyes, R.W. 1977, ARA&A, 15 363

Thanks to the MPCDF Raven/Cobra clusters for computational resources, and the open-source Free-EoS.